Novel Insights into Combating Cancer Chemotherapy Resistance Using a Plasmonic Nanocarrier: Enhancing Drug Sensitiveness and Accumulation Simultaneously with Localized Mild Photothermal Stimulus of Femtosecond Pulsed Laser

Liming Wang, Xiaoying Lin, Jing Wang, Zhijian Hu, Yinglu Ji, Shuai Hou, Yuliang Zhao, Xiaochun Wu, and Chunying Chen**

Chemotherapy resistance remains a large obstacle to successful clinical cancer therapy, mainly due to little accumulation and low sensitivity of drugs and the effective clinical strategy still lacks. Herein, a novel yet simple strategy to combat cancer drug resistance using the plasmonic feature-based photothermal properties is reported. Rather than directly killing cancer cells using nanoparticle-mediated hyperthermia, for the first time, localized plasmonic heating of gold nanorod at a mild laser power density can modulate the drug-resistance related genes. This photothermal effect triggers higher expression of heat shock factor (HSF-1) trimers and depresses the expression of P-glycoprotein (Pgp) and mutant p53. In turn, both drug accumulation in the breast cancer resistant cells (MCF-7/ADR) and their sensitiveness to drugs can be greatly enhanced. Considering the universality and feasibility of this strategy, it points out a new unique way to challenge drug resistance.

1. Introduction

Chemotherapeutic drugs such as doxorubicine (DOX) are widely used in cancer therapy but fail to kill cancers partly because cancer cells can develop multiple drug resistance (MDR) to survive toxic drugs.[1,2] Resistant cells evolve the ability to express several key genes that regulate drug uptake or efflux and increase their capacity to tolerate toxic drugs or escape apoptotic pathways.[3] Resistant cells develop a high expression of drug transporters such as P-glycoprotein (Pgp), also known as ABCB1 or MDR-1, that can effuse a wide variety of hydrophobic or amphipathic natural product drugs. In addition, resistant cells often undergo the mutation of pro-apoptosis genes such as TP53, whose mutated form induces anti-apoptosis capability in resistant cells and increases their tolerance to toxic drugs.[4] These properties are found in cells resistant to DOX; this resistance is a clinical challenge[5] because even high doses of DOX can barely depress resistant cancer cells and are accompanied by strong cardiotoxicity and other side effects.[2,6] It would thus be efficient to reverse resistance by simultaneously depressing Pgp and mutant p53 levels.

Recently, some strategies to resolve drug resistance[7] have used modulators,[3] small molecule inhibitors of efflux pathways,[8] nanomedicine,[9,10] siRNA,[11,12] and/or nanocarriers to improve drug accumulation,[13,14] and physical therapies such as X-ray radiation to promote regained sensitivity to drugs.[15,16] It is still a challenge to achieve a high delivery efficacy of siRNA plasmids of MDR-1 and drug carriers into cancer cells.[11] The physical therapies are tunable modes to sensitize cancer cells to drugs, but whether they can simultaneously regulate drug efflux and stimulate regained sensitivity to drugs is largely unknown. Nanocarriers, however, show great promise in cancer therapy due to their high loading efficiency, facile modification with target molecules, enhanced permeation and retention effects (EPR), and triggered drug release by multiple modes (such as pH, redox level, and light or heat).[17] Furthermore, nanotechnologies have a chance of improving therapy for resistant cells.[7] One nanoparticle that has emerged as a promising carrier for drugs, genes, and agents for thermal therapy and imaging is the gold nanorod (AuNR),[18–21] which possesses a unique shape and a size-dependent localized surface plasmon

Dr. L. Wang, X. Lin, J. Wang, Prof. Y. Zhao, Prof. C. Chen
CAS Key Laboratory for Biomedical Effects
of Nanomaterials and Nanosafety
National Center for Nanoscience and Technology
of China and Institute of High Energy Physics
Beijing, China
E-mail: chenchy@nanoctr.cn
X. Lin
Key Laboratory of Chinese Materia Medica
Heilongjiang University of Chinese Medicine
Ministry of Education
Harbin 150040, China
Dr. Z. Hu, Y. Ji, S. Hou, Prof. X. Wu
CAS Key Laboratory of Standardization
and Measurement for Nanotechnology
National Center for Nanoscience and Technology of China
Beijing 100190, China
E-mail: wuxc@nanoctr.cn

DOI: 10.1002/adfm.201400015

resonance (LSPR) feature.[21–23] At present, unprecedented control has been achieved in its quality and its localized SPR-enhanced properties in comparison with other shaped gold nanoparticles.[24] For instance, AuNRs of high quality have been obtained that have LSPR maxima at the first and second transparent windows of biological substances. Although localized photothermal effects of AuNRs can increase sensitivity of cancer cells to drugs, the detailed mechanism has remained elusive.[18,25,26] Meanwhile, whether photothermal effects can sensitize resistant cells or combat the nature of resistance is unknown. In addition, mesoporous silica shells around AuNRs can not only provide a large surface area for loading drugs such as DOX, but also maintain the optical properties of discrete AuNRs, which are critical to light-driven processes. Uncontrolled aggregation of AuNRs will result in significant change in the LSPR features, and may thus greatly diminish the positive effects of a photo-triggered strategy or even cause its complete failure. Our recent work has shown that AuNRs can selectively kill tumor cells, and that AuNR-based mesoporous silica nanocarriers (Au@SiO_2) can serve as integral nanoplatforms for simultaneous thermal and chemotherapies to kill cancer cells, and also allow concurrent fluorescence imaging.[18,27]

Here, we report that a dual functional nanoplatform of Au@SiO_2 particles can inhibit the growth of resistant breast cancer cells (MCF-7/ADR) by overcoming resistance pathways and increasing sensitivity to DOX due to the photothermal effects of AuNRs. We show that drug carriers can circumvent membrane transport protein Pgp-mediated DOX efflux by internalizing and accumulating DOX in lysosomes. More importantly, the photothermal effect of Au@SiO_2 causes high and long-term expression of heat shock factor-1 (HSF-1) trimers to combat drug resistance. The HSF-1 trimers repress the NF-κB pathway, which mediates MDR-1/Pgp expression. In addition, light-converted heat triggers the degradation of mutant p53 in resistant cells, which enhances the sensitivity of those cells to DOX. Finally, we have employed the integrated platform Au@SiO_2-DOX together with photothermal effects to both deliver DOX and reverse cellular resistance, with the result that the growth of resistant cells was significantly inhibited. This strategy holds a promise in future applications to treatment of multiple resistant cancers whose resistance is based on Pgp and mutant p53, and it will guide the design of functional nanoplatforms in cancer therapy.

2. Results and Discussion

2.1. Characterization of Au@SiO_2 Nanocarriers

AuNRs and spherical gold nanoparticles (AuNPs)-based mesoporous nanocarriers were prepared according to previously published methods.[18] Both the size and the shape are important parameters for photothermal conversion of AuNRs inside the cells by mediating the cellular uptake and accumulation of AuNRs and tuning their optical absorption properties under laser irradiation.[21,25,28,29] A proper aspect ratio is required for efficiently photothermal conversion during thermal therapy. AuNRs have a transverse plasmon peak at ≈520 nm and a longitudinal plasmon peak in the absorption spectra. The strongest light absorption occurs at the LP peak position that is determined by the aspect ratio rather than the size of AuNRs. Here, we tuned the aspect ratio to achieve an optimal photothermal conversion efficiency by using Au@SiO_2 and AuNPs@SiO_2, which are rod-like and sphere-like NPs with aspect ratios of ≈3.2 and ≈1, respectively. Dynamic light scattering data showed that the mean sizes of AuNPs and AuNPs@SiO_2 are 45.8 ± 1.7 nm and 105 ± 0.5 nm suggesting a 29.6 nm thickness of the silica layer (Supporting Information, Table S1). TEM images showed that the mean length and width are 61.8 ± 1.9 nm and 19.2 ± 0.9 nm for AuNRs and those for Au@SiO_2 are 98.3 ± 3.8 nm and 69.7 ± 2.5 nm. The thickness of silica layer in the longitudinal and transversal directions is 18.3 nm and 25.3 nm, respectively (**Figure 1**a). The silica layer increased the hydrodynamic size and changed the positive surface charges to negative ones (Supporting Information, Table S1), as shown by TEM images (Supporting Information, Figure S1a). Electrostatic adsorption was employed to load DOX inside the mesoporous shell, which also reversed the surface charges of the nanocarrier to positive due to the surface adsorption of DOX. The UV-Vis-NIR absorption spectra showed that the LSPR of AuNRs, Au@SiO_2, and Au@SiO_2-DOX were ≈760 nm, 780 nm, and 790 nm in the NIR region, respectively. In contrast, AuNPs and AuNPs@SiO_2 had a maximum absorbance around 530 nm (Figure 1b), suggesting that AuNR-based nanocarriers show a much better response to NIR light than AuNP-based ones. Upon femtosecond pulse laser irradiation of Au@SiO_2, a majority of NIR energy turns to heat (Figure 1c,d) whereas a tiny part is emitted and produces LSPR-enhanced two-photon fluorescence (Supporting Information, Figure S2).

We used MCF-7 cells, a human breast cancer cell line, and a DOX resistant one, MCF-7/ADR, to evaluate whether the photothermal effects of Au@SiO_2 can affect cellular responses to DOX. The two types of cells responded to DOX differently based on a CCK-8 assay. The toxicity of DOX to MCF-7 cells was dependent on dose and time. These cells were sensitive to DOX, and fewer than 10% of the cells survived for 48 h in 5 μM DOX (Figure 1f). However, MCF-7/ADR cells exhibited decreased viability that depended on dose and time only when the DOX dose was above 10 μM. When they were incubated with 5 μM DOX for 24 h, cell viability was nearly unchanged. After 48 h, cell viabilities of MCF-7/ADR cells were less sensitive to dose and seemed to be identical even at concentrations as high as 60 or 120 μM. This viability indicated that these cells were resistant to DOX (Figure 1g). The DOX dose at 1 μM was enough to decrease MCF-7 cell viability to (27.8 ± 1)% at 72 h, while for MCF-7/ADR cells a much higher dose of about 30–120 μM was required to achieve that goal. The half-maximal inhibitory concentration (IC_{50}) at 24 h easily showed the sensitivity of cells to DOX: The DOX IC_{50} of MCF-7 was about 5.2 μM whereas that for MCF-7/ADR was ≈158 μM (**Table 1**). Furthermore, we found that Au@SiO_2 had negligible effects on the viability of MCF-7/ADR cells below 60 μg mL^{-1}, a dose equivalent to 20 μM DOX (Supporting Information, Figure S3).

2.2. The Photothermal Effects of Au@SiO_2 and Increased Sensitivity to DOX

We next investigated the photothermal conversion of Au@SiO_2 with a femtosecond pulsed laser providing a high density

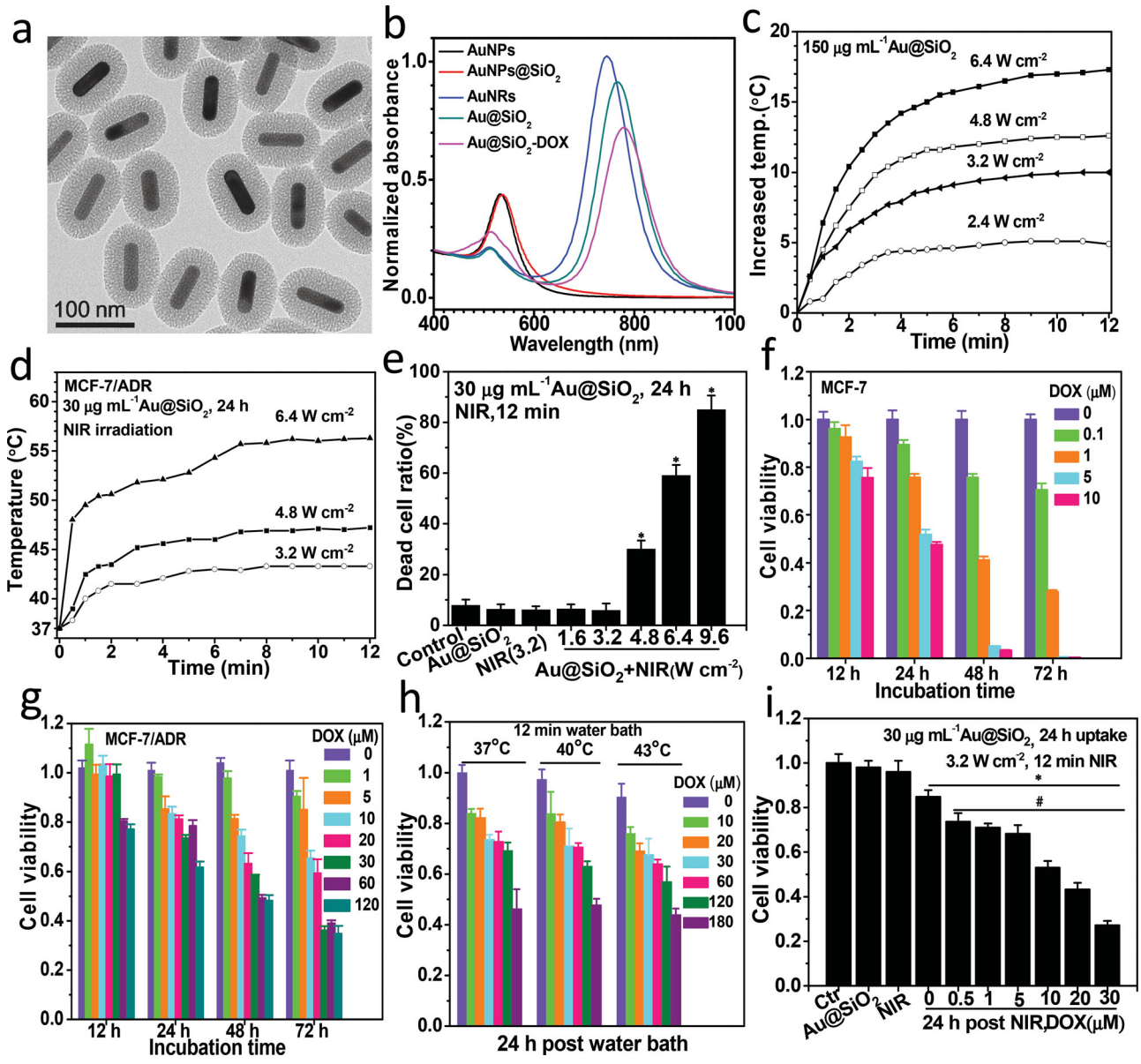

Figure 1. The characterization of $Au@SiO_2$, the photothermal effect induced by fs-pulse laser irradiation, and its direct effect on overcoming resistance of MCF-7/ADR cells to DOX. a) TEM image of $Au@SiO_2$ nanocarrier. b) Compared to AuNPs and $AuNPs@SiO_2$, the unique optical absorption properties of AuNRs and the mesoporous silica coated-nanocarriers including $Au@SiO_2$, and $Au@SiO_2$-DOX within the near infrared region, determined by UV-Vis-NIR spectroscopy. c–e) Under 780 nm fs-laser irradiation at a series of power densities, the changes in temperature of $Au@SiO_2$ solution (c) and that of MCF-7/ADR cell pellets after a 24 h incubation with 30 μg mL^{-1} $Au@SiO_2$ in complete cell culture medium (d), and thermal impact on dead cell ratio determined by CCK-8 assay (e). f,g) Dose-dependent cytotoxicity of DOX on MCF-7 and MCF-7/ADR cells. h, i) The influences of two thermal approaches on cell sensitivity to DOX: a water bath at 40 °C or 43 °C, and 780 nm fs-pulse laser irradiation at 3.2 W cm^{-2} for 12 min. Before NIR irradiation, MCF-7/ADR cells were exposed to 30 μg mL^{-1} $Au@SiO_2$ in complete cell culture medium for 24 h. Each data point (e–i) is shown as a mean value and standard deviation, $n = 3$. Significant differences in cell viabilities ($p < 0.05$) between control and treated cells are marked with an asterisk (*). After NIR irradiation, significant differences in cell viabilities ($p < 0.05$) between untreated cells and those treated with various doses of DOX are marked with a pound sign (#).

of photons. AuNRs in the core of $Au@SiO_2$ particles can efficiently absorb photons with energy centered at their LSPR peak and serve as highly efficient and localized heat sources. When it was irradiated with a 780 nm laser, $Au@SiO_2$ immediately converted light to heat to increase the temperature of $Au@SiO_2$ suspensions (about 150 μg mL^{-1}) (Figure 1c). The rise of temperature depended on the power density, and reached a plateau 5 min post-irradiation. However, for water or $AuNPs@SiO_2$ in solution under laser irradiation, the change in temperature was negligible due to low absorption efficiency (Supporting Information, Figure S6a). Cell pellets with internalized AuNRs changed temperature immediately, and the final equilibrium temperature depended on the irradiation power density (Figure 1d). A density of 3.2 W cm^{-2} was the critical energy

Table 1. The half maximal inhibitory concentrations (IC_{50}) of DOX for MCF-7 and MCF-7/ADR cells that are pretreated by NIR irradiation (3.2 W cm^{-2}) and water baths for 12 min, respectively. Before NIR irradiation, MCF-7/ADR cells were exposed to 30 μg mL^{-1} $Au@SiO_2$ in complete cell culture medium for 24 h.

Cell type	Pretreatment [°C]	IC_{50} [μM]
MCF-7	37	5.15
MCF-7/ADR	37	158.5
	40	145.2
	43	149.2
	$Au@SiO_2$+NIR	12.7

required to raise the overall temperature to 43 °C, a common temperature used in conventional thermal therapy. Irradiation at a higher density, 4.8 W cm^{-2} or more, promoted the temperature beyond 47 °C (Figure 1d) and led to more cell death, while 3.2 W cm^{-2} induced negligible cell death, as confirmed by the Live-Dead assay and the statistical results of the dead cell ratio (Supporting Information Figure S4, Figure 1e). Meanwhile, neither $Au@SiO_2$ alone nor NIR laser irradiation alone resulted in obvious cell death.

Here, we showed that not only would tumor therapy benefit from acute hyperthermia from $Au@SiO_2$ using a high power density, but more importantly, the pulse light-converted localized heat under 3.2 W cm^{-2} irradiation, much gentler than acute hyperthermia, helped sensitize MCF-7/ADR cells to DOX. We compared NIR laser irradiation to a water bath as a source of heat to bring cells to the same final equilibrium temperature. After MCF-7/ADR cells were exposed to $Au@SiO_2$ at a safe dose (30 μg mL^{-1}) for 24 h (Supporting Information, Figure S3), the irradiation (780 nm fs pulsed laser, 3.2 W cm^{-2}, 10 min) significantly increased their sensitivity to DOX (Figure 1i). The viability of irradiated cells with internalized $Au@SiO_2$ decreased to (53 ± 3)% at 10 μM DOX and (27.1 ± 2)% at 30 μM DOX within 24 h, respectively. The IC_{50} of DOX dropped to 12.7 μM, one twelfth the value for unirradiated cells (Table 1), which suggests that fs pulsed light-induced photothermal effects can sensitize resistant cells to chemotherapy drugs. Meanwhile, a water bath maintained at either 40 °C or 43 °C within 12 min failed to improve the sensitivity of MCF-7/ADR cells to DOX based on cell viability (Figure 1h) or IC_{50} (Table 1).

2.3. The Uptake and Localization of $Au@SiO_2$

To understand the behavior of $Au@SiO_2$ and the possible mechanisms for mediating resistance, we studied its uptake and localization using inductively coupled plasma mass spectrometry (ICP-MS) and TEM images. Most of the $Au@SiO_2$ particles were located in lysosomes with an intact silica shell on the surface (**Figure 2**a,b). The uptake of $Au@SiO_2$ was determined in the form of gold content using ICP-MS. The uptake amount increased with time and dose and reached a maximum at 24 h, about 10-fold that at 1.5 h (Figure 2c).

2.4. The Reversal of DOX Resistance Using NIR Laser Irradiation

To understand the way in which photothermal effects sensitize resistant cells, we focused on the process of producing heat based on a single Au nanorod. The actual temperature of a single rod is hard to capture under irradiation. We therefore simulated the temporal and spatial profiles of heat from single AuNR upon fs laser irradiation (Supporting Information, Figure S10). A pulsed laser stimulus (about 80 fs with 12.5 ns interval) at employed laser densities produced a small temperature rise at the Au surface, and it decays very fast. Therefore, the photothermal response is due to the cumulative effect of many NRs and localized at the region with AuNRs. The cumulative heat diffusion from a large number of AuNRs and continued irradiation gradually increased the temperature of cells or $Au@SiO_2$ suspensions to 43 °C (Figure 2d). We believe this localized heat plays a unique role.

In resistant cells, low accumulation of DOX is a main reason for DOX's failure to inhibit growth. The level of accumulated DOX in resistant cells was much lower than that in MCF-7 cells (Supporting Information, Figure S5b) because the highly expressed Pgp on the MCF-7/ADR plasma membrane facilitates DOX efflux. With fluorescence, DOX can be determined by flow cytometry, and mean fluorescence intensity (MFI) per cell was measured to study DOX accumulation (Supporting Information Figure S5a). Importantly, after internalization of $Au@SiO_2$ and then NIR irradiation, the uptake of DOX in MCF-7/ADR cells increased ≈four- and ≈eight-fold at 6 h and 12 h, respectively, over that in control cells (Figure 2e). Meanwhile, neither irradiation nor $Au@SiO_2$ treatment alone increased DOX accumulation. In the case of $AuNPs@SiO_2$, irradiation neither sensitized MCF-7/ADR cells nor increased DOX accumulation (Supporting Information, Figure S7a,b) due to its low photothermal efficiency at 780 nm as discussed above (Figure 1b, Figure S1b, Supporting Information). Meanwhile, the thermal effects induced by a water bath failed to promote levels of intracellular DOX (Figure 2f). These results mean that neither the water bath nor irradiation with a low efficiency of light-heat conversion was useful in reversing DOX resistance. Therefore, pulse laser-triggered localized heat can combat resistance by both enhancing sensitization to DOX and increasing DOX accumulation.

2.5. The Photothermal Effect Downregulates DOX Resistance Pathways

We next investigated possible mechanisms for the photothermally induced decrease in DOX resistance observed above. In MCF-7/ADR cells, RT-PCR showed that an irradiation density above 2.4 W cm^{-2} for light-converted heat significantly reduced the expression levels of the TP53 and MDR-1 genes (**Figure 3**a), which regulate DOX sensitivity and DOX exportation. To our surprise, treatment with short term water baths held at 43 °C and 45 °C failed to inhibit the expression of TP53 or MDR-1, and a water bath at 40 °C even promoted the expression of these two genes, an effect opposite to the result from laser irradiation (Figure 3b). These differences might result from the difference between the homothermal states in the water bath and the strong momentary

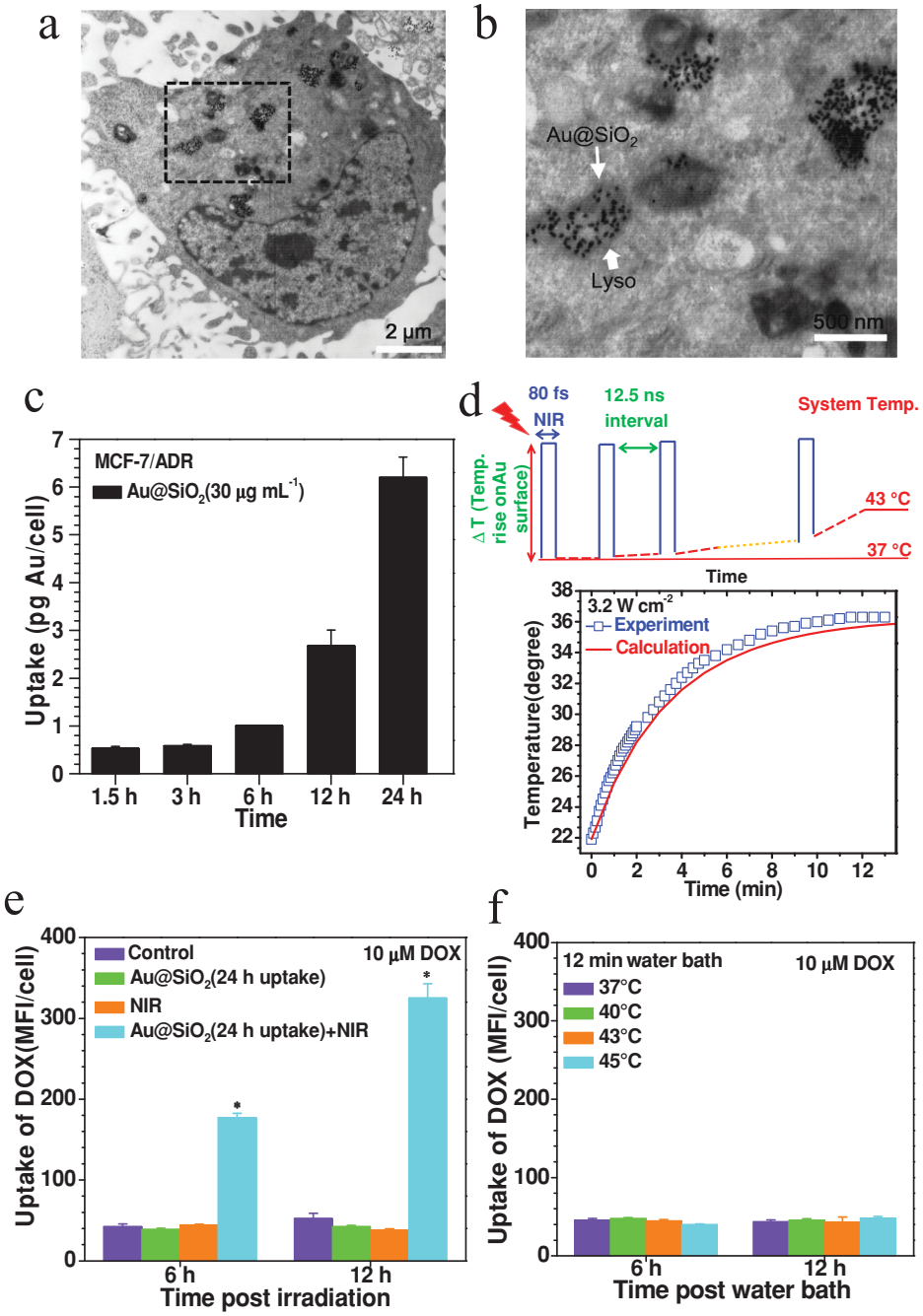

Figure 2. The improved drug accumulation in MCF-7/ADR cells and the state of Au@SiO_2 after NIR irradiation. a,b) TEM images showing the localization of Au@SiO_2 at the lysosomes and the coatings of silica shell structures on AuNRs inside a cell. Figures 2a represents a whole cell image and its zoomed insets are shown in Figure 2b. c) Time-dependent internalization of Au@SiO_2 at 30 μg mL^{-1} in complete cell culture medium within 24 h by MCF-7/ADR cells, determined by ICP-MS. d) In the upper schematic illustration, the generation and diffusion of the pulsed thermal effect is a localized heat around the AuNRs, which is driven by the change in Au surface temperature (ΔT). The cumulative heat leads to an increased equilibrium temperature for the system (the cells or the suspension of AuNRs). And theoretical simulation to show laser-induced heat of Au@SiO_2 and the coincidence of calculated and experimental results of the increase in equilibrium temperature of AuNR suspension when irradiation under a 3.2 W cm^{-2} power density of 780 nm laser. e) Improved DOX uptake for 6 h and 12 h after pretreatment with NIR irradiation. For control, MCF-7/ADR cells were directly incubated with 10 μM DOX in complete medium and measured by flow cytometry. For the Au@SiO_2 and Au@SiO_2+NIR groups, MCF-7/ADR cells were pre-treated with 30 μg mL^{-1} Au@SiO_2 for 24 h in the complete cell culture medium followed by laser irradiation at 3.2 W cm^{-2} for 12 min or not. For the NIR group, MCF-7/ADR cells were irradiated by an NIR laser without exposure to Au@SiO_2. f) No changes in DOX uptake by MCF-7/ADR cells for 6 h and 12 h after pre-immersion in a water bath at 37, 40, 43, and 45 °C for 12 min. All the data points are shown as mean value and standard deviation, $n = 3$. Significant differences ($p < 0.05$) between control and treated cells are marked with asterisks (*).

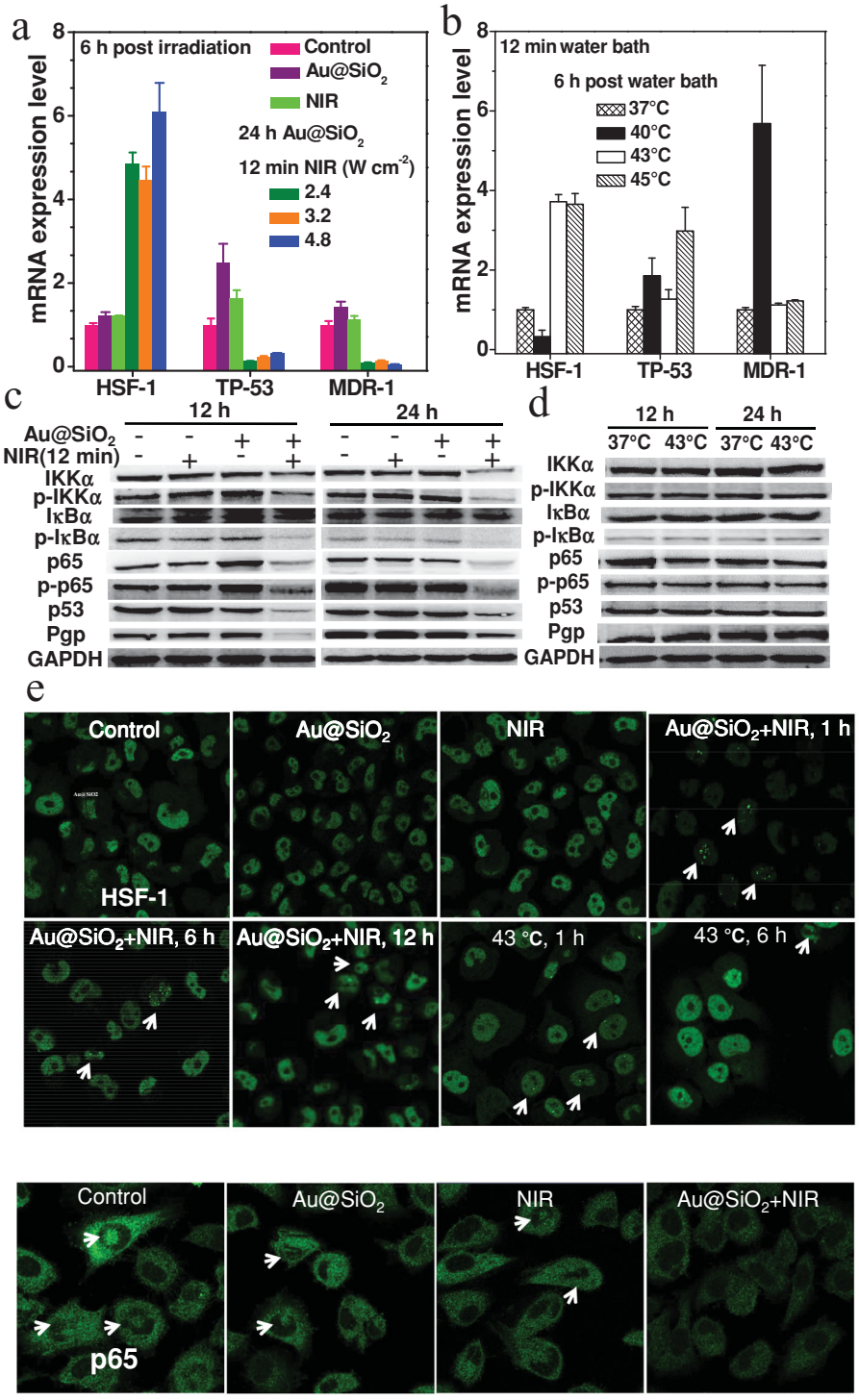

Figure 3. The influence of thermal effects on the molecular nature of drug resistance of MCF-7/ADR cells induced by NIR irradiation. a) Changes (folds) in transcription levels of three genes, HSF-1, TP53, and MDR-1, related to DOX resistance after treatment for 6 h as shown by RT-PCR. MCF-7/ADR cells were treated with NIR (3.2 W cm^{-2}, 12 min), Au@SiO_2 (after 24 h uptake of Au@SiO_2 at 30 μg mL^{-1}), and Au@SiO_2+NIR (after 24 h uptake of Au@SiO_2 at 30 μg mL^{-1}, and then irradiated for 12 min at the indicated power density). b) Changed folds of transcription levels of the same genes 6 h post-water bath at 37, 40, 43, and 45 °C for 12 min as measured by RT-PCR. c) Western blots of the impact of thermal treatment (24 h uptake of Au@SiO_2 at 30 μg mL^{-1}, then 12 min NIR irradiation under 3.2 W cm^{-2}) on the expression of key proteins that regulate the NF-κB pathway and resistance to DOX, 12 h and 24 h post-irradiation. The major proteins for the NF-κB pathway include IKKα, IκBα, p65, and their phosphorylated forms such as p-IKKα, p-IκBα, p-p65); their downstream proteins related to DOX resistance are p53 and Pgp. d) The impact of a water bath (at 43 °C, 12 min) on the same proteins 12 h and 24 h-post treatment. The reference protein was GAPDH. e) Confocal microscopic images of the different expression of HSF-1 trimer aggregates as functional HSF-1 protein within the nucleus, at different timepost-thermal stimulus by NIR irradiation or water bath. f) The differences in the expression of p65 and its translocation into nucleus 12 h post-NIR irradiation.

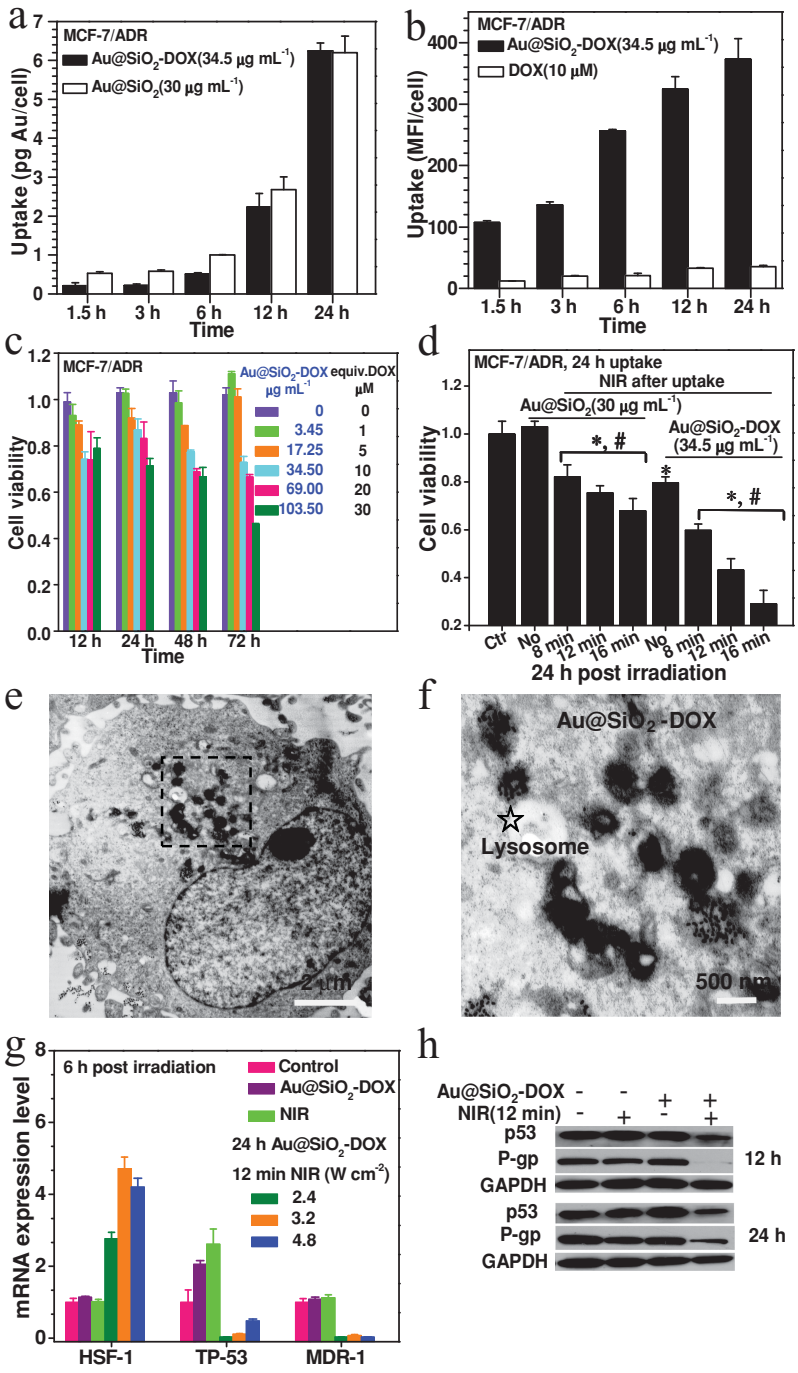

Figure 4. Using thermal effects of Au@SiO_2-DOX to inhibit the growth of MCF-7/ADR cells by combating DOX resistance and triggering DOX release. a) Time-dependent internalization of Au@SiO_2 and Au@SiO_2-DOX at a 10 μM DOX-equivalent dose within 24 h, shown as amount of Au per cell, as measured with ICP-MS. The dose of 34.5 μg mL^{-1} Au@SiO_2-DOX or 30 μg mL^{-1} Au@SiO_2 can be considered equal to a 10 μM equivalent DOX dose. b) Accumulated DOX when MCF-7/ADR cells were incubated with 10 μM DOX and the equivalent dose of Au@SiO_2-DOX within 24 h, as determined by the mean fluorescence intensity of a single cell using flow cytometry. c) Dose and time-dependent effects of Au@SiO_2-DOX on MCF-7/ADR cell viability. The dose of Au@SiO_2-DOX is described as the mass concentration (weight/weight ratio) and as the mole concentration of DOX within Au@SiO_2-DOX, respectively. d) After incubation with 34.5 μg mL^{-1} Au@SiO_2-DOX and 30 μg mL^{-1} Au@SiO_2 for 24 h, the thermal effects of both nanocarriers on cell viabilities 24 h post-irradiation, as measured by the CCK-8 assay. e, f) The localization of Au@SiO_2-DOX in the lysosomes of MCF-7/ADR cells after 24 h incubation. g,h) The influence of thermal treatment on both the transcription level (mRNA) of key resistance-related genes, including HSF-1, TP53, and MDR-1, and the expression of major resistance-related proteins such as p53 and Pgp after NIR irradiation. Each data point is shown as mean value and standard deviation, $n = 3$. Significant differences ($p < 0.05$) between control and treated cells are marked with asterisks (*). After 24 h uptake of Au@SiO_2 and Au@SiO_2-DOX, significant differences in cell viabilities ($p < 0.05$) between irradiated and unirradiated cells for different times are marked with pound signs (#).

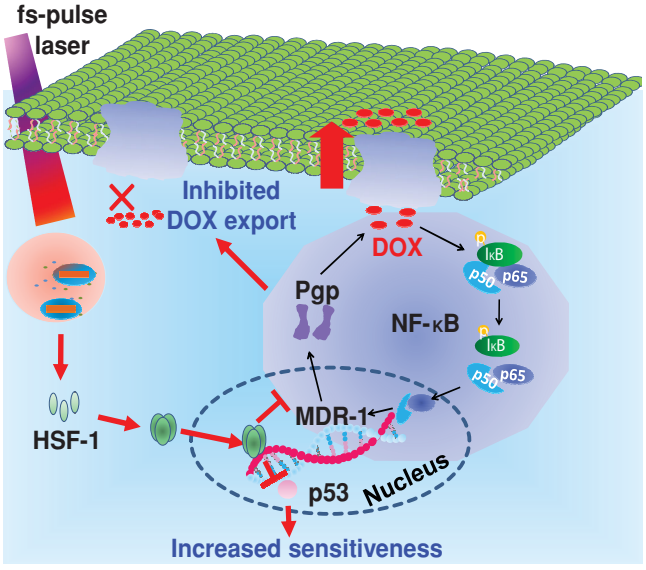

Figure 5. Mechanism of the reversal of drug resistance of cancer cells under fs-pulse laser irradiation. Both accumulated mutant p53 protein and activated NF-κB pathway contribute to the gain in resistance of breast cancer cells to DOX. Mutant p53 results in less sensitivity to toxic chemotherapeutic drugs, while NF-κB activates the expression of the MDR-1 gene and Pgp protein to export DOX. Nevertheless, the reversal of DOX resistance can be realized using mild photothermal therapy under fs-pulse laser. Intracellular Au@SiO_2 can produce pulsed hyperthermia to induce the formation of HSF-1 trimer to modulate the nature of resistant cells. The formed HSF-1 trimer can inhibit the expression of mutant p53 to increase the sensitiveness to DOX and repress the NF-κB pathway to reduce the expression of exporter Pgp, which in turn will increase the drug accumulation. Therefore, fs-pulsed laser irradiation can provide a novel and promising strategy to combat drug resistance with the aid of a multifunctional nanocarrier (Au@SiO_2) and triggered photothermal effects.

localized hyperthermia following irradiation. The heat is produced from repeated irradiation pulses (80 fs irradiation in each 12.5 ns interval) and the instaneous spreading of the surface heat to the envrionmental. Moreover, thermal effects induced by both modes can increase the expression of heat shock factor-1 (HSF-1), which serves as a sensor to respond to heat stimuli. But the momentary spike in heat was able to trigger HSF-1 expression much more effectively than the water bath at 40 °C. These results indicate that the two thermal modes result in distinct effects on the expression of genes closely related to resistance

Next, Western blotting was used to study the expression of resistance-related proteins in DOX-resistant MCF-7/ADR cells. Thermal effects from NIR irradiation significantly repressed the expression of p53 and Pgp proteins (Figure 3c). After treatment with a water bath at 43 °C, the expression of p53 and Pgp protein did not show any obvious changes (Figure 3d), and DOX resistance thus did not decreased (Figure 1h). Though p53 serves as a tumor suppressor gene to suppress surviving cancer cells, the major form present in resistant cancer cells is mutant p53. Mutant p53 does not exhibit the function of suppressing survivors, but rather increases resistance to apoptosis.[30–34] The result of NIR irradiation thus suggests that the sensitivity of MCF-7/ADR to DOX was improved because the resistant cells lost their anti-apoptosis ability when the level of mutated p53 protein was greatly reduced (Figure 3d). The other major effect of NIR irradiation, decreased expression of Pgp, will prevent efflux of DOX, which will increase DOX accumulation and lead to a higher DOX concentration, also resulting in more effective chemotherapy.

It is known that the transcription factor NF-κB plays an important role in activating the expression of the MDR-1 gene and inducing the development of drug resistance.[33,34] NF-κB is composed of homo or heterodimers such as the complex of RelA (p65) with NF-κB1 (p65/p50).[35,36] Inhibitors of NF-κB (IκB) located in the cytoplasm will bind to p65/p50 to form a complex that prevents the translocation of p65/p50 heterodimers to the nucleus. Phosphorylation of IκB by phosphorylated IκB kinase (p-IKK) will trigger IκB ubiquitination and degradation through proteasomes, which helps release p65/p50 from the complex. Then, the p65/p50 heterodimer translocates to the nucleus and binds to regulatory regions in promoters and enhancers to stimulate transcription of target genes for anti-apoptosis such as MDR-1.[35,36]

The IKK complex can induce canonical activation of the NF-κB p65/p50 heterodimer to trigger anti-apoptotic pathways.[37] Here, we studied the expression of major molecules that mediate the NF-κB pathway in MCF-7/ADR cells. Photothermal therapy depressed the expression of IKKα and phosphorylated IKKα (p-IKKα) (Figure 3c), suggesting that it may block an upstream part of the NF-κB pathway. The depressed expression of p-IKKα resulted in a decreased level of p-IκB and ultimately attenuated the translocation to and accumulation of functional NF-κB (p65/p50 dimers) in the nucleus, as supported by the immunofluorescence of p65 (Figure 3f). In addition, NIR irradiation repressed the expression of p65 and p-p65 (Figure 3c). Together with the depressed p-IKKα level, these results indicate that photothermal therapy substantially inhibits the activation of the NF-κB pathway. Conversely, a water bath at 43 °C for 12 min did not influence the expression of p65, p-p65, or p-IκB, which meant it did not intervene in the NF-κB pathway (Figure 3d).

Mutant p53 and NF-κB play important roles in the maintenance of multidrug resistance resulting from stress stimulus.[33,34] Conversely, HSF-1 reverses DOX resistance in resistant cells.[33] HSF-1 serves as a sensor to respond to heat stimulus. Activated HSF-1 forms homotrimers and translocates to the nucleus to bind to the promoters of target genes. As a transcription factor, the HSF-1 homotrimer competes with NF-κB to bind to the MDR-1 gene promoter region and antagonizes the expression of mutant p53.[34] Hence, we analyzed the HSF-1 homotrimer using microscopic fluorescence imaging. We found that photothermal treatment induced considerable formation of HSF-1 homotrimers at 1 h and that the homotrimers were retained for at least 12 h. However, many fewer HSF-1 homotrimers were observed after the 43 °C water bath, and they had nearly disappeared after 6 h (Figure 3e). Both thermal modes induced the formation of HSF-1 homotrimers, but their amounts and their lifetimes were quite different. This difference might result from the different ways of producing heat.

2.6. A Novel Application of Au@SiO_2-DOX to Combat DOX Resistance

In light of the above results, we extended our tests of Au@SiO_2 particles by loading them with DOX (Au@SiO_2-DOX) to see

whether they could overcome the drug resistance of tumor cells; the mesoporous SiO_2 shell can load a large amount of DOX, and the interior of the AuNRs not only provides an easy way to inducing hyperthermia and light–driven drug release,[18,26] but also offers SPR-enhanced imaging capabilities (such as the two-photon luminescence shown in Supporting Information Figure S2).[18] As a nanocarrier, Au@SiO_2-DOX increased the uptake and accumulation of DOX (**Figure 4**a,b) by loading DOX on the silica shell to prevent DOX efflux by Pgp. However, the nanoparticle carriers without photothermal treatment did not significantly improve the sensitivity of MCF-7/ADR cells to DOX (Figure 4c) because the DOX was released too slowly from the mesoporous SiO_2 shell to inhibit cell growth. In MCF-7/ADR cells over a 24 h period, Au@SiO_2-DOX resulted in an 8-fold increase in DOX accumulation over exposure to 10 μM DOX without nanoparticle carriers (Figure 4b). The reason for this increase is that Au@SiO_2-DOX could be internalized and distributed at endo/lysosomes (Figure 4e and 4f) rather than diffusing into the cytoplasm as DOX alone did. Meanwhile, the large uptake of DOX served to reduce cell viability with increasing dose and time.

As expected, photothermal treatment combined with Au@SiO_2-DOX helped reverse DOX resistance. With a 24 h incubation for internalization of the Au@SiO_2-DOX prior to irradiation, viability was reduced more in irradiated MCF-7/ADR cells than in un-irradiated ones 24 h after irradiation, with the reduction depending on irradiation time (Figure 4d). Within 24 h, MCF-7/ADR cells had taken up as much Au@SiO_2-DOX as they had Au@SiO_2 (Figure 4a). The photothermal influence of the two nanocarriers on cell death might thus be expected to be identical. However, photothermal effects also induce DOX release from nanocarriers.[18] Importantly, photothermal therapy with Au@SiO_2-DOX overcame resistance to DOX by the same mechanism as Au@SiO_2, by reducing mutant p53 and increasing DOX accumulation via depression of MDR-1 or Pgp levels (Figure 4g,h). Because irradiated Au@SiO_2 had smaller effects on cell death, Au@SiO_2-DOX must have induced cell death through both an increase in released DOX and improved sensitivity to DOX (Figure 4b,d). Photothermal therapy thus sensitized MCF-7/ADR cells to the released DOX and also reduced DOX efflux, which in time contributed to growth inhibition.

2.7. Discussion

Acquired DOX resistance comes mainly from drug efflux and direct suppression of apoptosis. Diminished DOX accumulation results from the elevated expression of a member of the ATP-binding cassette (ABC) transporter family, p-glycoprotein (Pgp). At least 40% of breast cancers show elevated Pgp or MDR-1 expression during chemotherapy[5] or hormonal therapy,[38] which increases drug efflux and decreases retained DOX, ultimately leading to chemotherapy failure.[2,3,38]

In order to circumvent drug resistance, chemical inhibitors or modulators have been developed to target MDR-1 or Pgp, including the calcium channel blocker verapamil, cyclosporin A, GF-902128, PSC-833, VX-710, and others; however, these have been unsuccessful in clinical trials because they lack selectivity.[3,39] Both resistant cells and normal tissues such as the liver and kidney abundantly express MDR-1/Pgp. Due to poor selectivity, inhibitors may also target normal cells, and this non-specific inhibition may result in cytotoxicity.[39,40] Furthermore, even though silencing the MDR-1 gene using siRNA techniques can reduce Pgp expression and increase the susceptibility of cancer cells,[11,41] the delivery of siRNA and its controllable release and stability in vivo are still challenges. Meanwhile, mesoporous nanocarriers have a large surface area available for loading drugs and increasing DOX uptake by internalization, and protective shells to encapsulate DOX to avoid drug efflux by Pgp.[11,13] Moreover, ultrasound-induced hyperthermia (41–45 °C) combined with the Pgp modulator PSC-833 improved the therapeutic efficiency slightly. This kind of hyperthermia only elevated DOX accumulation and increased cytotoxicity 2-fold because it enhanced the drug entry rate rather than depressing Ppg expression.[42,43] Combination with radiotherapy or hyperthermia can sensitize cancer cells to drugs and inhibit the growth of cancer cells, mainly based on the apoptosis genes, but information about the drug efflux pathway is lacking.[25,43–48] An efficient strategy is thus required to overcome DOX resistance by both increasing sensitivity and depressing DOX efflux.

Herein, the mesoporous silica-coated AuNRs (Au@SiO_2) serve as a powerful tool to overcome resistance of cancer cells by simultaneously realizing increased sensitivity and depressed DOX efflux. The present report represents an exciting advance utilizing a physical therapy, photothermal therapy, to reverse drug resistance. This method efficiently represses the expression of MDR-1/Pgp in resistant breast cancer cells and increases the accumulation of DOX inside cells. After loading with DOX, irradiated Au@SiO_2-DOX not only reversed resistance but also produced a synergistic effect that sensitized cells to the released DOX. The modes to produce the heat stimulus are quite different for water baths and pulsed laser-triggered hyperthermia, which resulted in different effects on resistance reversal. An 80 fs pulse within a 12.5 ns interval is effective at producing hyperthermia during each pulsed irradiation. Simulation results showed that a single irradiated gold nanorod produces local and instant heat. As the temperature within the rod drops by heat diffusion, the absorbed heat gradually elevates the environmental temperature to about 43 °C. By controlling the power density of the irradiation, the temperature can be maintained at around 43 °C, the optimum temperature. By comparison, a water bath retains a constant temperature system at 43 °C to stimulate cells. These strikingly different modes of stimulating cells result in the different observed effects on reversal of resistance.

Photothermal therapy produces a strong stimulus to MCF-7/ADR cells and can cause cell death under controlled power densities. Photothermally induced momentary hyperthermia greatly elevates the levels of HSF-1 homotrimers. Heat shock factors are members of the stress protein family, which responds to stress or stimulus.[49] HSF-1 is a classic transcription factor that has a low expression in resistant cells, but whose increased expression helps reverse DOX resistance.[33] HSF-1 trimers compete with NF-κB to bind to the promoter region of the MDR-1 gene to depress resistance to DOX.[50] As a stress-related transcription factor, NF-κB binds to the MDR-1

gene promoter (CAAT) and activates the MDR-1 gene, contributing to the development of drug resistance.[34,50] Thus, as photothermal therapy significantly increases HSF-1 expression and induces the copius formation of HSF-1 homotrimers, high levels of HSF-1 trimers repress the expression and activity of NF-κB, which in turn depresses MDR-1/Pgp expression and allows DOX to accumulate.

In addition to increasing DOX accumulation, photothermal therapy significantly improves sensitivity to DOX. NF-κB is an anti-apoptosis transcription factor in the presence of chemotherapeutic drugs and other stimuli such as tumor necrosis factor-α, and thus the inhibition of NF-κB activation can promote apoptosis and improve cellular sensitivity to drugs. This effect coincides with the result of reduced expression of mutant p53 after photothermal therapy. p53 is a tumor repressor gene that mediates cancer cell apoptosis during chemotherapy. However, in resistant cancers, the majority of p53 exists in the mutant form and competes with wild type p53.[30,31,38] The mutant type silences the p53-correlated apoptosis pathway, which makes resistant cells less sensitive to toxic drugs.[32,51] The reduced expression of mutated p53 in MCF-7/ADR cells could thus enhance their sensitivity to DOX.[52] The reduced expression of mutant p53 is partly derived from HSF-1 activation. Overall, we have shown that the pulsed laser-triggered photothermal effects of Au@SiO_2 nanocarriers overcome DOX resistance by forming and activating HSF-1 trimers, which efficiently depress the expression of (DOX-exporting) Pgp and improve sensitivity to DOX.

3. Conclusion

In summary, we present a novel function of Au@SiO_2: to combat chemotherapy drug resistance of breast cancer cells through fs pulsed laser-induced photothermal effects. We have shown that internalized Au@SiO_2 in lysosomes converts light to instant hyperthermia and, compared to a water bath treatment, stimulates resistant cells to express more heat shock factor protein and form more HSF-1 monotrimer to translocate to the nucleus. Elevated HSF-1 trimers block the NF-κB pathway, which in turn depresses the expression of both the exporter Pgp on the plasma membrane and mutant p53. Therefore, photothermal therapy rather than a water bath helps to overcome DOX resistance and kill tumor cells efficiently by increasing the load of accumulated DOX and improving sensitivity to it (**Figure 5**). Finally, the combination of DOX loading and photothermal treatment with Au@SiO_2 in the form of Au@SiO_2-DOX can improve the efficiency of inhibiting resistance in MCF-7/ADR cells because it not only triggers DOX release controllably but also largely combats resistance to DOX. This integrated nanoplatform combining photothermal therapy with chemotherapy promises to inhibit a wide range of resistant cancers whose resistance relies on Pgp and mutant p53. Considering the ever-growing applications of laser technology in the medical field, we believe that this novel and convenient physical strategy based on a highly controlled photothermal effect of plasmonic nanostructures will demonstrate its potential for combating drug resistance in cancer therapy.

Supporting Information

Supporting Information is available from the Wiley Online Library or from the author. It includes the experimental section and materials, the characterization of Au@SiO_2 and AuNPs@SiO_2, the key parameters related to the laser-induced photothermal effect, the influences of Au@SiO_2 on cell viability under NIR irradiation or not, the uptake process of DOX, the thermal impact of NIR irradiation on DOX uptake and the sensitivity of cells to DOX, the temporal and spatial diffusion process of surface heat on a single AuNR after irradiation.

Acknowledgements

This work was financially supported by the National Basic Research Program of China (2012CB934000, 2010CB934004, and 2011CB933401), the International Science & Technology Cooperation Program of China (2013DFG32340), the Major Equipment Program (2011YQ030134) from Ministry of Science Technology of China, the National Natural Science Foundation of China (11205166, 31070854, and 21320102003), and German Federal Ministry of Education and Research (BMBF 0315773A). The authors appreciated Dr. Luru Dai at NCNST for two-photon fluorescence experiment.

Received: January 3, 2014
Revised: February 6, 2014
Published online: March 24, 2014

[1] M. M. Gottesman, *Annu. Rev. Med.* **2002**, *53*, 615.
[2] M. M. Gottesman, T. Fojo, S. E. Bates, *Nat. Rev. Cancer* **2002**, *2*, 48.
[3] G. Szakács, J. K. Paterson, J. A. Ludwig, C. Booth-Genthe, M. M. Gottesman, *Nat. Rev. Drug Discovery* **2006**, *5*, 219.
[4] R. Brosh, V. Rotter, *Nat. Rev. Cancer* **2009**, *9*, 701.
[5] A. U. Buzdar, C. Marcus, T. L. Smith, G. R. Blumenschein, *Cancer* **1985**, *55*, 2761.
[6] S. Wadler, J. Z. Fuks, P. H. Wiernik, *J. Clin. Pharmacol.* **1987**, *27*, 357.
[7] A. Shapira, Y. D. Livney, H. J. Broxterman, Y. G. Assaraf, *Drug Resist. Update* **2011**, *14*, 150.
[8] E. A. Dubikovskay, S. H. Thorne, T. H. Pillow, C. H. Contag, P. A. Wender, *Proc. Natl. Acad. Sci. U.S.A.* **2008**, *105*, 12129.
[9] Y. Min, C. Q. Mao, S. Chen, G. Ma, J. Wang, Y. Liu, *Angew. Chem. Int. Ed.* **2012**, *51*, 6742.
[10] X. J. Liang, H. Meng, Y. Wang, H. He, J. Meng, J. Lu, P. C. Wang, Y. Zhao, X. Gao, B. Sun, C. Chen, G. Xing, D. Shen, M. M. Gottesm, Y. Wu, J. J. Yin, L. Jia, *Proc. Natl. Acad. Sci. U.S.A.* **2010**, *107*, 7449.
[11] H. Meng, M. Liong, T. Xia, Z. Li, Z. Ji, J. I. Zink, A. E. Nel, *ACS Nano* **2010**, *4*, 4539.
[12] H. Meng, W. X. Mai, H. Zhang, M. Xue, T. Xia, S. Lin, X. Wang, Y. Zhao, Z. Ji, J. I. Zink, A. E. Nel, *ACS Nano* **2013**, *7*, 994.
[13] Y. Gao, Y. Chen, X. Ji, X. He, Q. Yin, Z. Zhang, J. Shi, Y. Li, *ACS Nano* **2011**, *5*, 9788.
[14] F. Wang, Y. C. Wang, S. Dou, M. H. Xiong, T. M. Sun, J. Wang, *ACS Nano* **2011**, *5*, 3679.
[15] G. D. Wilson, S. M. Bentzen, P. M. Harari, *Semin. Rad. Oncol.* **2006**, *16*, 2.
[16] B. W. Robinson, D. S. Shewach, *Clin. Cancer Res.* **2001**, *7*, 2581.
[17] D. Peer, J. M. Karp, S. Hong, O. C. Farokhzad, R. Margalit, R. Langer, *Nat. Nano.* **2007**, *2*, 751.
[18] Z. Zhang, L. Wang, J. Wang, X. Jiang, X. Li, Z. Hu, Y. Ji, X. Wu, C. Chen, *Adv. Mater.* **2012**, *24*, 1418.
[19] L. Xu, Y. Liu, Z. Chen, W. Li, Y. Liu, L. Wang, Y. Liu, X. Wu, Y. Ji, Y. Zhao, L. Ma, Y. Shao, C. Chen, *Nano Lett.* **2012**, *12*, 2003.

[20] A. F. Bagley, S. Hill, G. S. Rogers, S. N. Bhatia, *ACS Nano* **2013**, *7*, 8089.
[21] H. Chen, L. Shao, Q. Lia, J. Wang, *Chem. Soc. Rev.* **2013**, *42*, 2679.
[22] E. C. Dreaden, A. M. Alkilany, X. Huang, C. J. Murphy, M. A. El-Sayed, *Chem. Soc. Rev.* **2011**, *41*, 2740.
[23] A. M. Alkilany, L. B. Thompson, S. P. Boulos, P. N. Sisco, C. J. Murphy, *Adv. Drug Delivery Rev.* **2012**, *64*, 190.
[24] R. Rodríguez-Oliveros, J. A. Sánchez-Gil, *Opt. Express* **2012**, *20*, 621.
[25] T. S. Hauck, T. L. Jennings, T. Yatsenko, J. C. Kumaradas, W. C. W. Chan, *Adv. Mater.* **2008**, *20*, 3832.
[26] S. Shen, H. Tang, X. Zhang, J. Ren, Z. Pang, D. Wang, H. Gao, Y. Qian, X. Jiang, W. Yang, *Biomaterials* **2013**, *34*, 3150.
[27] L. Wang, Y. Liu, W. Li, X. Jiang, Y. Ji, X. Wu, L. Xu, Y. Qiu, K. Zhao, T. Wei, Y. Li, Y. Zhao, C. Chen, *Nano Lett.* **2011**, *11*, 772.
[28] Y. Qiu, Y. Liu, L. Wang, L. Xu, R. Bai, Y. Ji, X. Wu, Y. Zhao, Y. Li, C. Chen, *Biomaterials* **2010**, *31*, 7606.
[29] Z. Zhang, J. Wang, C. Chen, *Adv. Mater.* **2013**, *25*, 3869.
[30] M. Olivier, A. Langerod, P. Carrieri, J. Bergh, S. Klaar, J. Eyfjord, C. Theillet, C. Rodriguez, R. Lidereau, I. Bieche, J. Varley, Y. Bignon, N. Uhrhammer, R. Winqvist, A. Jukkola-Vuorinen, D. Niederacher, S. Kato, C. Ishioka, P. Hainaut, A. L. Borresen-Dale, *Clin. Cancer Res.* **2006**, *12*, 1157.
[31] A. Willis, E. J. Jung, T. Wakefield, X. Chen, *Oncogene* **2004**, *23*, 2330.
[32] J. V. Thottassery, G. P. Zambetti, K. Arimori, E. G. Schuetz, J. D. Schuetz, *Proc. Natl. Acad. Sci. U.S.A.* **1997**, *94*, 11037.
[33] R. Kanagasabai, K. Krishnamurthy, L. J. Druhan, G. Ilangovan, *J. Biol. Chem.* **2011**, *286*, 33289.
[34] K. Krishnamurthy, K. Vedam, R. Kanagasabai, L. J. Druhan, G. Ilangovan, *Proc. Natl. Acad. Sci. U.S.A.* **2012**, *109*, 9023.
[35] M. Karin, A. Lin, *Nat. Immunol.* **2002**, *3*, 221.
[36] A. S. Baldwin Jr., *Ann. Rev. Immunol.* **1996**, *14*, 649.
[37] S. K. Srivastava, K. V. Ramana, *Exp. Eye Res.* **2009**, *88*, 2.
[38] M. Lacroix, R. A. Toillon, G. Leclercq, *Endocr. Relat. Cancer* **2006**, *13*, 293.
[39] R. Krishna, L. D. Mayer, *Eur.J. Pharm. Sci.* **2000**, *11*, 265.
[40] B. I. Sikic, *Semin. Hematol.* **1997**, *34*, 40.
[41] X. B. Xiong, A. Lavasanifar, *ACS Nano* **2011**, *5*, 5202.
[42] Y. Liu, C. W. Cho, X. Yan, T. K. Henthorn, K. O. Lillehei, W. N. Cobb, K. Y. Ng, *Pharm. Res.* **2001**, *18*, 1255.
[43] Y. Liu, K. Lillehei, W. N. Cobb, U. Christians, K. Y. Ng, *Biochem. Biophys. Res. Commun.* **2001**, *289*, 62.
[44] G. M. Hahn, J. Braun, I. Har-Kedar, *Proc. Natl. Acad. Sci. U.S.A.* **1975**, *72*, 937.
[45] P. Wardman, *Clin. Oncol.* **2007**, *19*, 397.
[46] W. Walther, F. Arlt, I. Fichtner, J. Aumann, U. Stein, P. M. Schlag, *Mol. Cancer Ther.* **2007**, *6*, 236.
[47] J. You, R. Shao, X. Wei, S. Gupta, C. Li, *Small* **2010**, *6*, 1022.
[48] A. Rossi, S. Ciafrè, M. Balsamo, P. Pierimarchi, M. G. Santoro, *Cancer Res.* **2006**, *66*, 7678.
[49] M. Åkerfelt, R. I. Morimoto, L. Sistonen, *Nat. Rev. Mol. Cell Biol.* **2010**, *11*, 545.
[50] B. Ogretmen, A. R. Safa, *Biochemistry* **1999**, *38*, 2189.
[51] G. Schneider, A. Henrich, G. Greiner, V. Wolf, A. Lovas, M. Wieczorek, T. Wagner, S. Reichardt, A. von Werder, R. Schmid, *Oncogene* **2010**, *29*, 2795.
[52] S. Fan, M. L. Smith, D. J. Rivert, D. Duba, Q. Zhan, K. W. Kohn, A. J. Fornace, P. M. O'Connor, *Cancer Res.* **1995**, *55*, 1649.